Fuel 158 (2015) 443–450

Contents lists available at ScienceDirect

Fuel

journal homepage: www.elsevier.com/locate/fuel

Laminar flame propagation and ignition properties of premixed iso-octane/air with hydrogen addition

Zisen Li [a], Wang Han [a], Dong Liu [b], Zheng Chen [a,*]

[a] SKLTCS, Department of Mechanics and Engineering Science, College of Engineering, Peking University, Beijing 100871, China
[b] School of Energy and Power Engineering, Nanjing University of Science and Technology, Nanjing 210094, China

HIGHLIGHTS

- Flame propagation and ignition properties of iC_8H_{18}/H_2/air are studied.
- Effects of hydrogen addition on laminar flame speed are examined.
- The Markstein length changes non-monotonically with hydrogen blending.
- Small amount of hydrogen addition greatly reduces minimum ignition energy.

ARTICLE INFO

Article history:
Received 9 March 2015
Received in revised form 23 May 2015
Accepted 29 May 2015
Available online 3 June 2015

Keywords:
Iso-octane/hydrogen blends
Laminar flame speed
Markstein length
Minimum ignition energy

ABSTRACT

Numerical simulations of one-dimensional planar and spherical flame propagation of iso-octane/hydrogen/air mixtures at different equivalence ratios and hydrogen blending levels are conducted considering detailed chemistry. Our focus is on the effects of hydrogen addition on laminar flame propagation and ignition of iso-octane/air mixtures. Specifically, the laminar flame speed, Markstein length, and minimum ignition energy of iso-octane/hydrogen binary fuel blends are investigated. The laminar flame speed is found to increase first slightly and then exponentially with the molar ratio of hydrogen in the iso-octane/hydrogen binary fuel blends. However, a nearly linear trend is observed when the mass ratio instead of molar ratio of hydrogen blending is considered. Similar trend holds for hydrogen addition to other hydrocarbon fuels such as methane and propane. The thermal and chemical effects involved in laminar flame speed enhancement by hydrogen addition are quantified and it is found that the chemical effect prevails over the thermal effect. Unlike the laminar flame speed, the Markstein length is found to change non-monotonically with hydrogen blending ratio. Blending hydrogen to iso-octane/air and blending iso-octane to hydrogen/air both promote diffusive-thermal instability. Moreover, the minimum ignition energy of iso-octane/air is shown to be reduced by a small amount of hydrogen addition, especially for the fuel lean case. When the hydrogen blending molar ratio is above 60%, the minimum ignition energy is found to be insensitive to hydrogen addition.

1. Introduction

Binary fuel blends can be used in internal combustion engines (ICEs) to achieve high-efficiency and low-emission since ignition and flame propagation properties can be controlled through adjusting the fuel blending ratio [1–3]. On account of its advantageous combustion properties such as high combustion rate and broad flammability limit range, hydrogen can serve as a blending fuel to other fuels [4]. For example, natural gas/hydrogen mixtures can be utilized in ICEs (see the review paper [5] and references therein). Ma et al. [6,7] have systematically investigated the thermal efficiency and emission characteristics of natural gas engines with hydrogen enrichment. Due to its promising application in ICEs, a lot of investigations on basic combustion properties of hydrogen/methane binary fuel blends have been conducted including ignition [8,9], laminar flame speed [10–12], flame instability [13,14], flame structure [15,16] and so on.

Recently, Ji et al. [17–19] have proposed to use hybrid hydrogen-gasoline spark-ignition engine (SIE) to achieve lower emission and higher thermal efficiency than pure gasoline-fueled SIE. Therefore, a systematic investigation of fundamental combustion characteristic of gasoline with hydrogen addition is of practical interests. Since iso-octane (iC_8H_{18}) has been extensively utilized as

* Corresponding author. Tel.: +86 10 62766232.
E-mail address: cz@pku.edu.cn (Z. Chen).

http://dx.doi.org/10.1016/j.fuel.2015.05.070
0016-2361/

a surrogate for gasoline, a binary fuel blend of hydrogen and iso-octane is considered in the present study. In the literature, there are only a few fundamental studies on iso-octane/hydrogen binary fuel blends. Tahtouh et al. [20] and Bouvet et al. [21] experimentally measured the laminar flame speeds of iC_8H_{18}/H_2/air mixtures and found that large proportion of hydrogen in the binary fuel blends leads to the increase of laminar flame speed. Mandilas et al. [22] experimentally assessed the effects of hydrogen addition on the behaviors of laminar and turbulent iso-octane flames. They found that hydrogen addition promotes laminar flame instability and doubles the turbulent flame speed. Jain et al. [23] simulated the homogeneous ignition process of iC_8H_{18}/H_2/air mixtures and found that the ignition is controlled by different reaction paths as the amount of hydrogen addition changes.

The influence of hydrogen addition on the laminar flame speed, Markstein length and minimum ignition energy of iC_8H_{18}/H_2 binary fuel blends is still not well understood. The laminar flame speed is one of the most important parameters of a combustible mixture and it determines the fuel consumption rate in ICEs. Therefore, the first objective is to examine the hydrogen addition effects on laminar flame speed of iso-octane/air. Moreover, the correlation between the laminar flame speed and hydrogen blending level is investigated.

Another important parameter of a combustible mixture is the Markstein length, which quantifies the sensitivity of local flame speed change to external stretch rate and determines the diffusive–thermal flame instability. It is closely related to the onset of instability during flame propagation, which will cause flame acceleration [24–26] and potentially induce knock in engines [27]. Besides, in engine simulations, Markstein length is an input parameter in certain premixed turbulent combustion modeling which considers the influence of local stretch or curvature on flame propagation speed [28]. Bouvet et al. [21] and Mandilas et al. [22] measured the Markstein length of iC_8H_{18}/H_2/air mixture. However, Markstein length measurement is very sensitive to extrapolation and the uncertainty in Markstein length measurement is very large (one order of magnitude larger than that of laminar case) [29]. Hence the second objective of this work is to obtain Markstein length of iC_8H_{18}/H_2/air mixtures through numerical simulation and to find how the Markstein length changes with hydrogen addition.

The last objective of this work is to investigate the ignition process of iso-octane/hydrogen binary fuel blends with the emphasis put on the minimum ignition energy (MIE). To our knowledge, there is no study on the MIE of iC_8H_{18}/H_2/air mixtures in the literature. Here the MIE is calculated and different regions for the variation of MIE with hydrogen blending ratio are identified.

2. Numerical method

The combustion properties of premixed iC_8H_{18}/H_2/air mixtures are studied through numerical simulation considering detailed chemistry. The composition of the unburned pre-mixture is specified according to the expression of $\phi[(1-\alpha)iC_8H_{18}+\alpha H_2]+(12.5-12\alpha)(O_2+3.76N_2)$, in which ϕ is the equivalence ratio and α represents the hydrogen volume/mole fraction in iC_8H_{18}/H_2 binary fuel blends. The mass fraction of hydrogen in iC_8H_{18}/H_2 binary fuel blends is denoted by β. Here we only consider the initial pressure of 1 atm and initial temperature of 423 K. It is noted that the current thermodynamic state of 1 atm and 423 K is quite different from engine-relevant burning condition. This is a limitation of the present study. Further effort is needed to investigate the influences of high pressure, high temperature, and the existence of dilution on the combustion of iC_8H_{18}/H_2 binary fuel blends.

Two premixed flame configurations for iC_8H_{18}/H_2/air mixtures are considered: one is the unstretched planar flame, and the other is the propagating spherical flame with positive stretch. The CHEMKIN–PREMIX code [30] is used to simulate planar flame propagation and to obtain the laminar flame speeds of the binary fuel with different composition (ϕ = 0.8, 1.0, 1.2 and α = 0.0–1.0). In all cases, the detailed chemistry and multicomponent transportation properties are considered.

The Markstein length and MIE of iC_8H_{18}/H_2/air mixtures are determined from flame front history of propagating spherical flames, which is simulated using the in-house code, A-SURF [31–33]. A-SURF solves one-dimensional conservation equations for reactive flow [31–33]. Adaptive mesh refinement is used to efficiently and accurately resolve the propagating flame front. The CHEMKIN libraries [34,35] are used in A-SURF to calculate the reaction rates and thermodynamic and transportation properties. A-SURF has been used in ignition and flame propagation studies (e.g., [36,37,60]). More specifics (governing equations and numerical schemes) can be found in Refs. [31–33].

The spherical flame is initialized by imposing an energy deposition within a given time duration with space distribution specified as Ref. [38]

$$q_{ig}(r,t)=\begin{cases}\frac{E_{ig}}{\pi^{1.5}r_{ig}^3\tau_{ig}}\exp\left[-\left(\frac{r}{r_{ig}}\right)^2\right] & \text{if } t<\tau_{ig}\\ 0 & \text{if } t\geq\tau_{ig}\end{cases} \quad (1)$$

where E_{ig} represents the total amount of energy input, τ_{ig}, the duration of the energy release, and r_{ig}, the radius of ignition source. The size and duration of the energy source are specified as τ_{ig} = 0.2 ms and r_{ig} = 0.2 mm, respectively [38]. The MIE is obtained based on trial-and-error procedure with relative error less than 1%.

In all simulations, the length of the computational domain is 100 cm. To obtain Markstein length, only the temporal trajectory data of flame front within the range $1.5 \leqslant R_f \leqslant 2.0$ cm are used in order to eliminate the influences of ignition [31] and pressure rise [32,39]. It is noted that nearly the same results are obtained for $1.0 \leqslant R_f \leqslant 1.5$ cm and thereby the extrapolation results are not sensitive to the flame radius range used in data processing. The flame front is defined as the position of maximum heat release rate. According to the time evolution of flame front position, $R_f = R_f(t)$, the Markstein length can be linearly extrapolated based on the following expression [40]

$$S_b = S_b^0 - L_b\kappa \quad (2)$$

The normalized formulation of Eq. (2) is derived as

$$S_b/S_b^0 = 1 - Ma'Ka \quad (3)$$

where $Ka = \kappa\delta/S_u^0$ is the Karlovitz number; $Ma' = \sigma L_b/\delta$ the density-ratio weighted Markstein number; σ the density ratio; and δ the flame thickness.

In the literature there are several mechanisms developed for iso-octane (e.g., [41,42]). Here we use the high-temperature mechanism developed by Chaos et al. [41] which comprises 116 components and 754 elementary reactions. It was validated against ignition delay and laminar flame speed measurements [41]. Besides, it includes the hydrogen oxidation mechanism developed by Li et al. [43]. Therefore, it can be used to study the high-temperature combustion properties of iso-octane/hydrogen binary fuel blends.

3. Results and discussion

3.1. Laminar flame speed

Laminar flame speed, S_u^0, and adiabatic flame temperature, T_{ad}, of iC_8H_{18}/H_2/air mixtures are shown in Fig. 1. The experimental

results of Bouvet et al. [21] are also presented in Fig. 1(a). Good consistency between simulation and experimental data is observed, which indicates that the mechanism of Chaos et al. [41] can be used to study the high-temperature combustion properties of iC_8H_{18}/H_2 binary fuel blends. Both S_u^0 and T_{ad} are shown to increase monotonically with α. For each equivalence ratio, the change of the S_u^0 against α comprises two regimes: in the first regime with $\alpha < 0.8$, S_u^0 is insensitive to hydrogen addition and it only slightly increases with α ; and in the second regime with α approaching to unity (pure hydrogen), S_u^0 increases exponentially. Similar trend was also observed for other hydrogen blended fuels such as CH_4/H_2 [12] and C_3H_8/H_2 [21]. Such trend is caused by the large difference in molecular weight between H_2 and iC_8H_{18}: 80% hydrogen addition in volume only brings about 7% hydrogen addition in mass.

The effects of hydrogen addition on S_b^0 of different hydrocarbon fuels are quantitatively compared by introducing the following laminar flame speed increase due to increment of hydrogen content in a normalized form

$$S_{u,norm}^0(\alpha) = \frac{S_u^0(\alpha) - S_u^0(\alpha = 0)}{S_u^0(\alpha = 1) - S_u^0(\alpha = 0)} \quad (4)$$

in which $S_u^0(\alpha)$ represents the laminar flame speed at the blending level of α. $\alpha = 0$ and $\alpha = 1$ respectively represents pure fuel and pure hydrogen. Similar definition can also be introduced in terms of β, which denotes the hydrogen content in the binary fuel blends in mass fraction. The normalized laminar flame speeds of hydrogen blended methane, propane, and iso-octane (also from simulation [44] using PREMIX) are plotted in Fig. 2. In terms of volume fraction, exponential increase in $S_{u,norm}^0$ is observed in Fig. 2(a) when α is approaching to unity. Moreover, at the same hydrogen blending level α, $S_{u,norm}^0$ is shown to decrease with the carbon number. This is because the ratio of the molecular weight of hydrocarbon fuel to that of hydrogen increases with the carbon number. The change of $S_{u,norm}^0$ with β shown in Fig. 2(b) exhibits nearly a linear correlation and it does not depend on the carbon number. Therefore, for hydrocarbon/hydrogen binary fuel blends, the relative increase in laminar flame speed due to hydrogen blending can be approximated by the correlation of $S_{u,norm}^0 \approx \beta$.

Previous studies suggested there exist certain correlations between S_b and the concentration of some key radicals such as H or OH radicals. For example, Yamamoto et al. [45] found linearity between S_b^0 and maximum OH radical concentration. However, our results for iC_8H_{18}/H_2 binary fuel blends in Fig. 3(a) indicates that S_b^0 does not increase linearly with the maximum OH radical concentration. Cheng et al. [46] suggested that the linear relationship exists between S_b^0 and the maximum summation of H and OH molar fractions, i.e., $[X_H + X_{OH}]_{max}$. In Fig. 3(b), similar linear

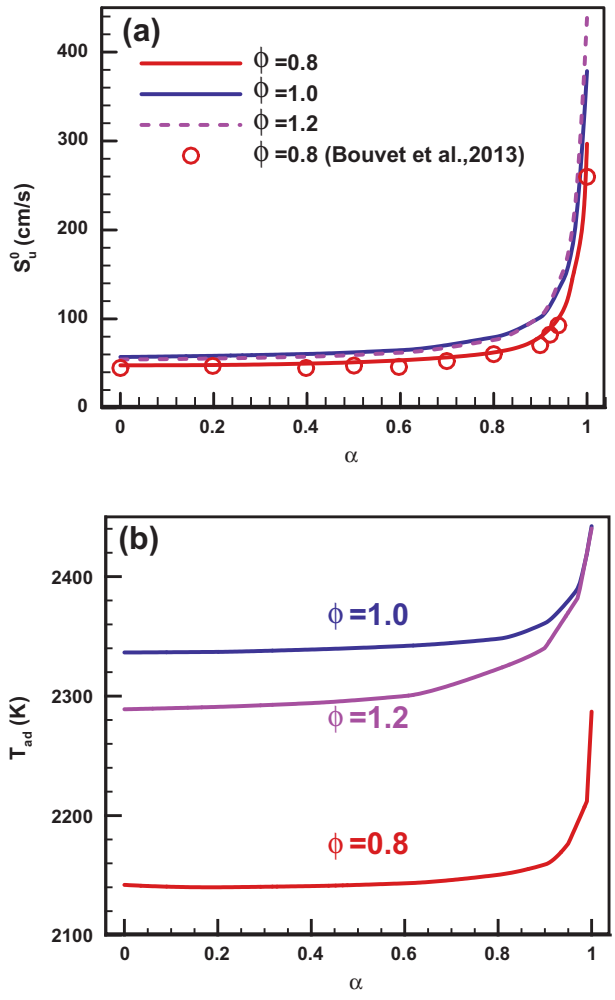

Fig. 1. (a) Laminar flame speed and (b) adiabatic flame temperature of H_2/iC_8H_{18}/air mixtures at $T_u = 423$ K and $P = 1$ atm.

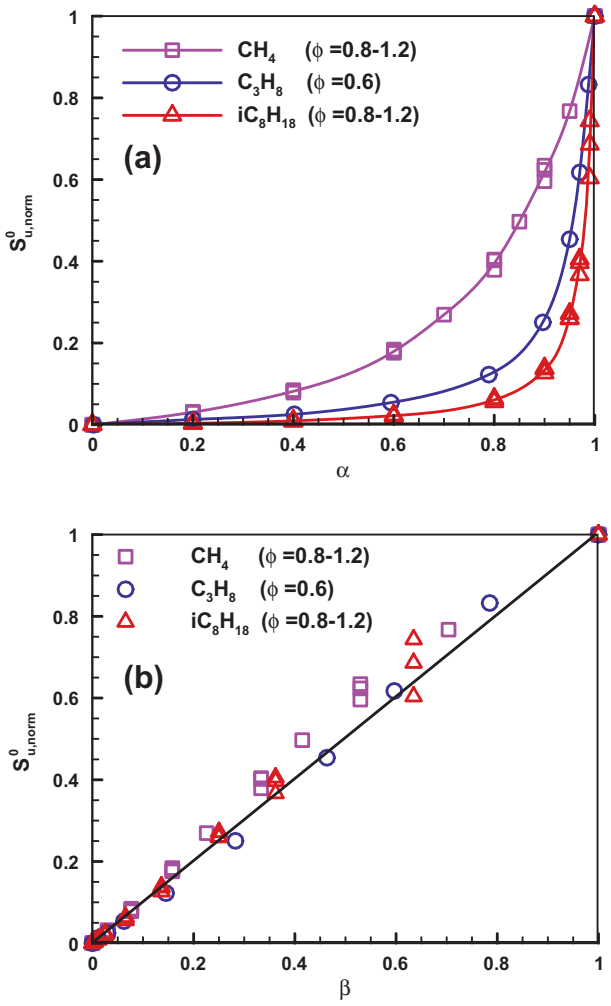

Fig. 2. Normalized laminar flame speed as a function of hydrogen blending level in terms of volume fraction (a) and mass fraction (b).

relationship is also observed for iC_8H_{18}/H_2 binary fuel blends. However, the slope in Fig. 3(b) is 7495 cm/s for iC_8H_{18}/H_2 blending fuel, which is different from the value of 4114 cm/s for C_1–C_4 alkane fuel in Ref. [46]. Therefore, this slope depends on the type of fuel (blending); and further study is needed in order to get a universal correlation working for different fuels.

The increase in the laminar flame speed through hydrogen addition is caused by thermal effect due to the increase in the flame temperature (see Fig. 1(b)), chemical effect due to the reduction of chemical activation energy, and transport effect due to the high mobility of hydrogen [47]. Tang et al. [47] showed that the transport effect is relatively negligible. Therefore, here we only focus on the thermal and chemical effects. The following strategy, which was proposed by Wang et al. [48] and later applied for n-butane and iso-butane by Sung et al. [49], is taken to assess the individual contribution of thermal and chemical effects. The strategy is briefly described below and more details can be found in Ref. [49]. To assess the thermal effect, the baseline fuel (pure iC_8H_{18} without H_2 addition) mixture is adjusted by replacing part of the nitrogen with argon (which has smaller heat capacity) to make the adiabatic flame temperature to be the same as that of the hydrogen blended fuel. It is noted that the third-body collision coefficient of Ar slightly differs from that of N_2. However, the change of laminar flame speed caused by the change in third-body collision coefficient is within 1% and thereby it is negligible. We use $S^0_{u,T}(\alpha)$ to represent the laminar flame speed of the modified baseline fuel mixture. The contribution of thermal effect to laminar flame speed increase by hydrogen addition is quantified by

$$\Delta S^0_{u,therm} = \frac{S^0_{u,T}(\alpha) - S^0_u(\alpha = 0)}{S^0_u(\alpha) - S^0_u(\alpha = 0)} \quad (5)$$

where the numerator is the change of laminar flame speed caused by purely thermal effect and the denominator is the total change of laminar flame speed by hydrogen blending at the ratio of α. Similarly, for chemical effect, part of nitrogen is replaced with carbon dioxide (which has relatively large heat capacity) to make the adiabatic flame temperature of hydrogen blended fuel same as that of the pure iC_8H_{18}/air without hydrogen addition. The corresponding flame speed is denoted as $S^0_{u,C}(\alpha)$. The contribution of chemical effect to laminar flame speed increase by hydrogen addition is

$$\Delta S^0_{u,chem} = \frac{S^0_{u,C}(\alpha) - S^0_u(\alpha = 0)}{S^0_u(\alpha) - S^0_u(\alpha = 0)} \quad (6)$$

where the numerator is the change of laminar flame speed caused mainly by chemical effect and denominator is the total change of laminar flame speed by hydrogen blending at the ratio of α. Contributions of thermal and chemical effects to laminar flame speed increase at different α are shown in Fig. 4. It is seen that both thermal and chemical effects are pronounced and contribute to the flame speed enhancement. The laminar flame speed increase caused by chemical effect is about three times larger than that by thermal effect. Similar results are found for the case of $\phi = 0.8$ and $\phi = 1.2$.

Several key elementary reactions that contribute to the enhancement of laminar flame speed are identified through sensitivity analysis. The results are shown in Fig. 5. It is seen that the sensitivity coefficients of chain branching reaction, $HO_2 + H = OH + OH$, and chain propagating reaction, $H_2 + OH = H_2O + H$, increase significantly with hydrogen blending level. Alkyl radicals are generated both from H abstraction (a/b/c/d-C_8H_{17}) or C–H bond cleavage (t–iC_4H_9), or from the parent fuel due to thermal decomposition following isomerization and β-scission routes [41]. However, the influence of hydrogen addition on these reactions which include species of high carbon level (C_5–C_7) is not as significant as these of small carbon number. Therefore, laminar flame propagation is mainly enhanced by the basic H_2-related chain reactions for iC_8H_{18}/H_2 mixtures. Besides, it is noted that Fig. 5 shows that the sensitivity coefficient of reaction $H + O_2 = O + OH$ changes non-monotonically with hydrogen blending ratio. Unfortunately,

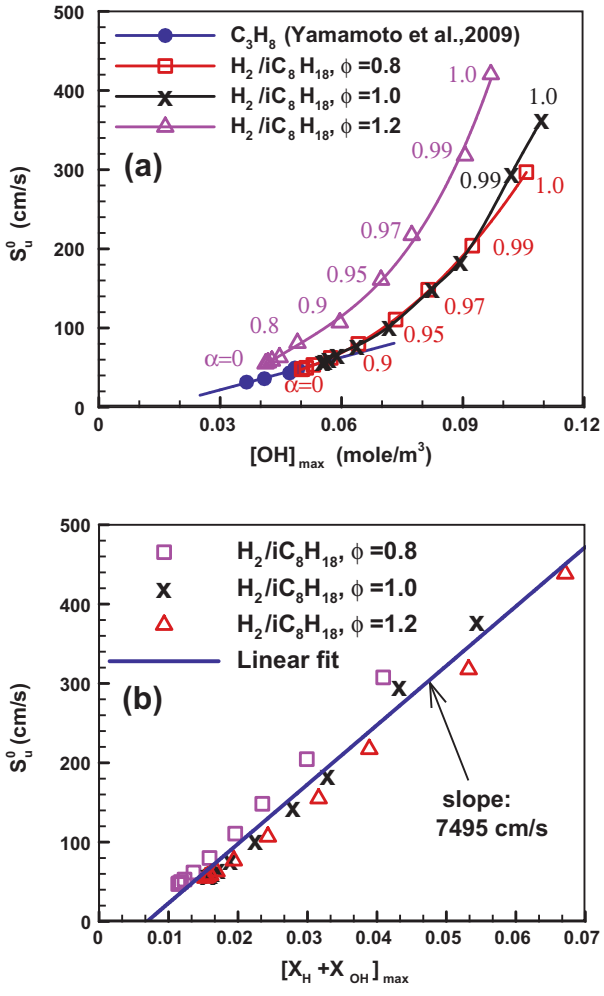

Fig. 3. Change of laminar flame speed with (a) maximum OH molar concentration (b) maximum mole fraction of H and OH. The results for C_3H_8/air mixtures from Yamamoto et al. [45] are also presented.

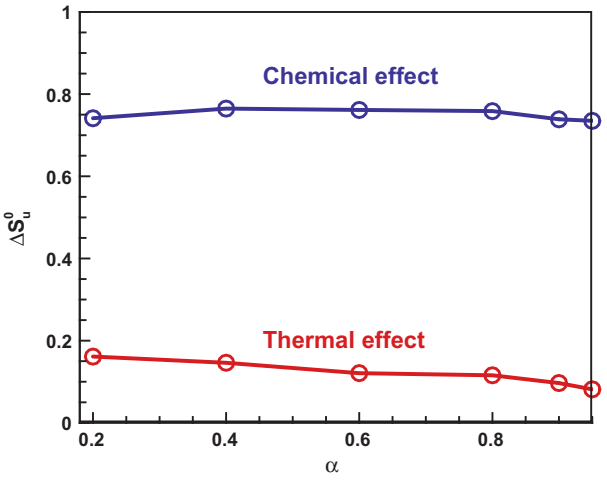

Fig. 4. Thermal and chemical effects of hydrogen addition on the laminar flame speeds of iC_8H_{18}/air mixtures ($\phi = 1.0$).

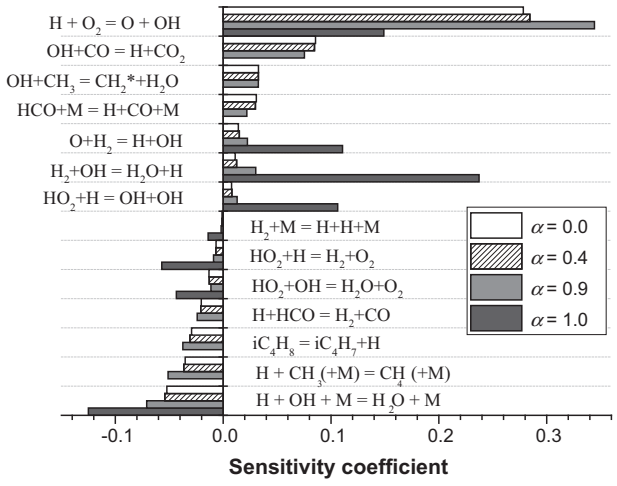

Fig. 5. Sensitivity of elementary reactions to laminar flame speeds of H_2/iC_8H_{18}/air mixtures.

we do not have a good explanation for such non-monotonic change.

Recently, several models have been proposed for the prediction of S_u^0 of binary fuel blends [44,50,51], which are summarized in Table 1. Other related references on such kind model development and application are [52–56]. Here the performances of these models with respect to the S_u^0 of iC_8H_{18}/H_2/air mixtures are evaluated. The result in Fig. 6 indicates that model II and model III can give accurate prediction of S_u^0 for iC_8H_{18}/H_2 binary fuel blends, and that great over-prediction is given by Model I. Therefore, only models II and III work for iC_8H_{18}/H_2. It is noted that there is a free parameter to be determined in Model III [44]. The free parameter c is determined by the requirement that at $\alpha = 0.6$ the laminar flame speed predicted by model III is equal to the PREMIX result. Model II has the advantage of being parameter free. Furthermore, model II was proved to work also for iso-octane/methanol and iso-octane/ethanol fuel under engine conditions [55].

3.2. Markstein length and minimum ignition energy

Propagation of spherical flames for iC_8H_{18}/H_2/air mixtures are numerically simulated by A-SURF so that the Markstein length and MIE are obtained. Fig. 7 shows the normalized flame speed as a function of Karlovitz number for stoichiometric iC_8H_{18}/H_2/air mixtures. Only the results among flame radius $1.5 \leqslant R_f \leqslant 2.0$ cm are presented so that the ignition effect at small flame radius and pressure rise at large flame radius can be avoided. There is a negative linearity between the stretched flame speed and the Karlovitz number. Therefore, positive Markstein length can be obtained from linear extrapolation based on Eq. (2).

The Markstein lengths of iC_8H_{18}/H_2 binary fuel blends are plotted in Fig. 8. The experimental data from Bouvet et al. [21] are also presented for comparison. Good agreement between simulation and experimental results is observed at $\alpha \geqslant 0.7$. However, the experimental results are lower than simulation results with linear

Table 1
Model for prediction of laminar flame speed for binary fuel blends.

Model	Formulation	Reference
I	$S_L(\phi, \alpha) = [\alpha/S_{L,H2}(\phi) + (1-\alpha)/S_{L,Fuel}(\phi)]^{-1}$	Di Sarli et al. [50]
II	$S_b^0 = \exp\left[\sum_{i=1}^{2} \tau_i \ln\left(S_{u,i}^0\right)\right]$	Hirasawa et al. [51]
III	$m_{mix}^2 = (Y_{1,u}m_1^2 + cY_{2,u}m_2^2)/(Y_{1,u} + cY_{2,u})$	Chen et al. [44]

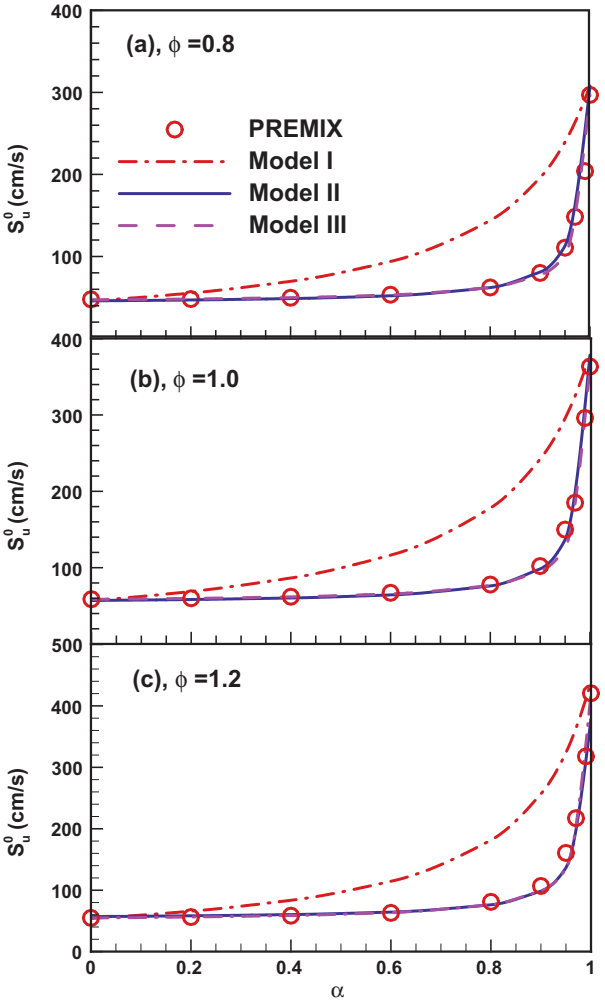

Fig. 6. Laminar flame speed of H_2/iC_8H_{18} binary fuel blends predicted by different models ($T_u = 423$ K, $P = 1$ atm). The prediction of model II is very close to that of model III so that these two lines are nearly overlapped.

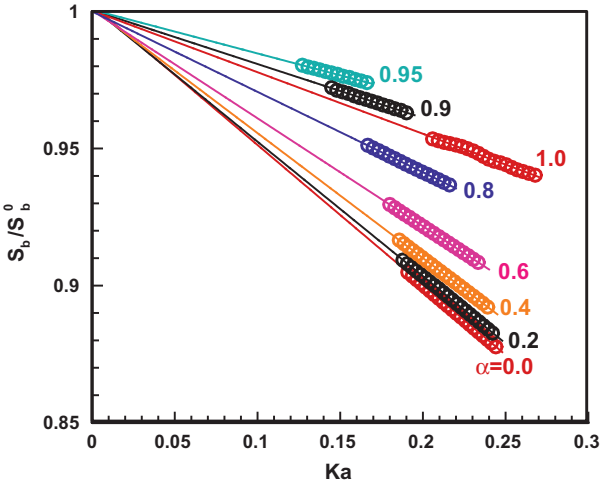

Fig. 7. Normalized flame propagation speed as a function of Karlovitz number for stoichiometric ($\phi = 1.0$) H_2/iC_8H_{18}/air mixtures at $T_u = 423$ K and $P = 1$ atm. Solid lines: linear extrapolation; symbols: simulation results.

extrapolation for $\alpha < 0.7$. The difference is due to the fact that Bouvet et al. [21] obtained the Markstein length from nonlinear extrapolation, which yields smaller values of Markstein length

than linear extrapolation [29]. This is demonstrated in Fig. 8 by the comparison between L_b from linear extrapolation (dash–dotted line) and that from nonlinear extrapolation (dash–dot–dotted line). The simulation results for all three equivalence ratios ($\phi = 0.8$, 1.0, and 1.2) indicate that the Markstein length varies non-monotonically with α. Either blending H_2 to iC_8H_{18}/air mixture ($0 \leqslant \alpha < 0.96$) or blending iC_8H_{18} to H_2/air mixture ($0.96 < \alpha \leqslant 1.0$) destabilizes the flame propagation and promotes its instability. This non-monotonic behavior predicted by simulation is in quantitative accordance with experimental results of iso-octane at $\phi = 0.8$ by Bouvet [21]. Similar trend was also observed for other hydrogen blended fuels such as CH_4/H_2 [12] and C_3H_8/H_2 [21]. As explained in [57], the non-monotonic variation in L_b with α is caused by the competitive change between Lewis number and Zel'dovich number.

The change of the MIE, E_{min}, of H_2/iC_8H_{18}/air mixtures as a function of hydrogen blending level, α, is shown in Fig. 9. The variation of E_{min} also contains two regimes: it firstly decreases greatly with hydrogen addition at $\alpha < 0.6$ and then becomes insensitive to hydrogen addition with E_{min} approaching to the value of pure hydrogen/air. When the hydrogen blending level is above 0.6, the ignition process is mainly controlled by hydrogen with high reactivity and mobility, and thereby the MIE is nearly constant. This can be further explained by looking through the unsteady ignition process as follows.

Figure 10(a) shows the change of flame propagation speed, S_b, with the stretch rate, κ, at $\phi = 0.8$ and $\alpha = 0.4$, for which the MIE lies between 0.216 mJ and 0.217 mJ. The spherical flame kernel is initially driven by the ignition energy decomposition (regime I), and then evolves to be unsteady transition regime II after the first turning point and normal flame propagation regime III after the second turning point [58]. In regime III, S_b changes linearly with the stretch rate at small κ and it approaches to the planar flame when the flame radius is large enough. Results of $E_{ig} = 0.216$ mJ and $E_{ig} = 0.217$ mJ show that the transition in regime II plays crucial role in ignition. Besides, increasing ignition energy (0.534 mJ) enhances both flame kernel initialization in regime I and transition in regime II.

The positive external stretch inhibits the flame propagation when the Lewis number of the deficient reactant is above unity. Enrichment of hydrogen into iso-octane/air mixture can enhance the flame propagation in regimes I and II: hydrogen addition can greatly promote radical generation and heat release from chemical reaction; and it can reduce the Lewis number. This fact is demonstrated by Fig. 10(b) which shows the normalized flame propagating speed as a function of normalized stretch rate for three different values of α. For each case, the ignition energy is set to

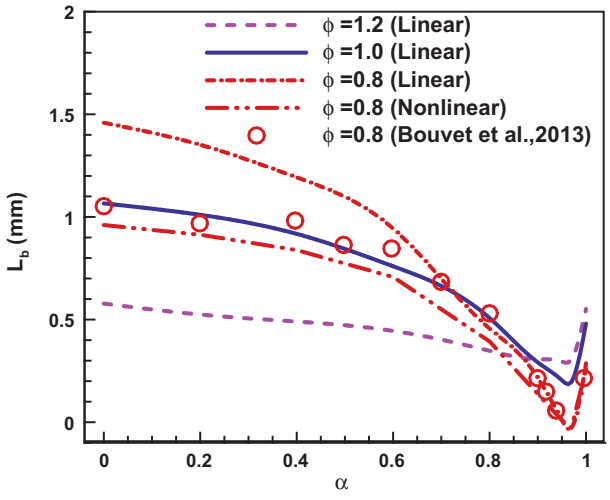

Fig. 8. Markstein length of H_2/iC_8H_{18} binary fuel blends. Solid line: computational results; empty symbols: experimental results by Bouvet et al. [21].

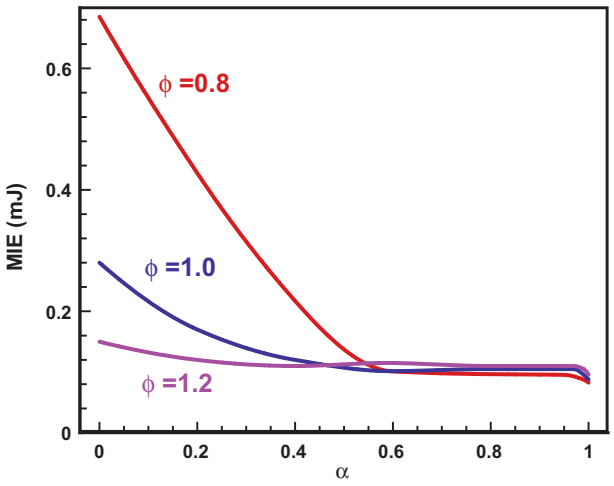

Fig. 9. Minimum ignition energy of H_2/iC_8H_{18}/air mixtures at $T_u = 423$ K and $P = 1$ atm.

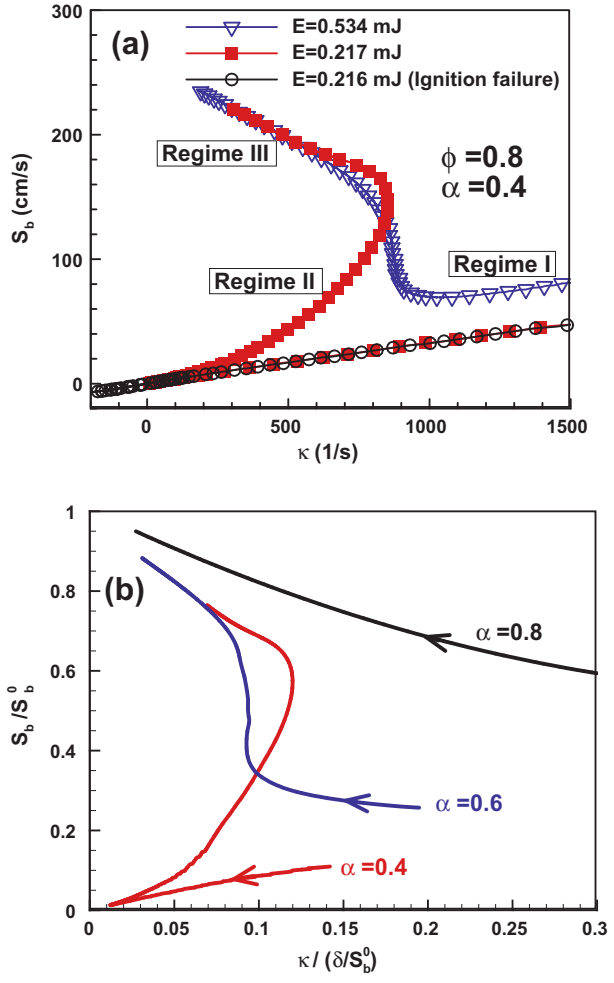

Fig. 10. Flame speed S_b as a function of stretch rate κ for iC_8H_{18}/H_2/air at $\varphi = 0.8$, $P = 1$ atm, and $T_u = 423$ K. (a) $\alpha = 0.4$ with different ignition energies; (b) $\alpha = 0.4$, 0.6, 0.8 with ignition energy slightly larger (<1%) than the corresponding MIE at each α.

be slightly larger (<1%) than MIE of each α to ensure successful ignition. It is seen that the propagation speed of the small ignition kernel (corresponding to large stretch rate) is greatly enhanced with the increase of hydrogen addition. Therefore, the MIE is greatly reduced by hydrogen addition when α is small ($\alpha < 0.6$). At the same hydrogen blending level, the MIE decreases with the increase of the equivalence ratio as shown in Fig. 9. This is due to the fact that the Markstein length decreases with the increase of equivalence ratio (see Fig. 8) and the MIE becomes smaller at lower value of L_b [36,59].

4. Conclusions

Planar and spherical propagating flames of premixed iC_8H_{18}/H_2/air mixtures are numerically simulated. Effects of hydrogen addition on the laminar flame speed S_u^0, Markstein length L_b, and minimum ignition energy E_{min} are examined. The main conclusions are:

(1) The change of S_u^0 with hydrogen blending level α contains two regions: in the first regime with $\alpha < 0.8$, S_u^0 only slightly increases with α in a linear manner; while, in the second regime with α approaching toward unity, S_u^0 increases exponentially with α. Different hydrogen blended hydrocarbon fuels (CH_4, C_3H_8, and iC_8H_{18}) are considered and the relative increment in laminar flame speed due to hydrogen blending is found to be approximately equal to the mass fraction of hydrogen in the fuel blends. Moreover, the chemical effect is shown to be predominant over thermal effect in the enhancement of S_u^0.

(2) The Markstein length of iso-octane/hydrogen binary fuel first decreases and then increases with the hydrogen blending level. Therefore, blending hydrogen to iso-octane or blending iso-octane to hydrogen can reduce the Markstein length and promote the diffusive-thermal instability. Hydrogen addition can greatly reduce the MIE at $\alpha < 0.6$. However, when the hydrogen blending level is above 0.6, the ignition is controlled by hydrogen with high mobility and reactivity and thereby the MIE is nearly constant.

Acknowledgements

The work was supported by National Natural Science Foundation of China (Nos. 51322602 and 51136005) and Jiangsu Provincial Natural Science Foundation of China (BK20140034).

References

[1] Lu X, Han D, Huang Z. Fuel design and management for the control of advanced compression-ignition combustion modes. Prog Energy Combust Sci 2011;37:741–83.
[2] Lü X, Hou Y, Zu L, Huang Z. Experimental study on the auto-ignition and combustion characteristics in the homogeneous charge compression ignition (HCCI) combustion operation with ethanol/n-heptane blend fuels by port injection. Fuel 2006;85:2622–31.
[3] Reitz RD, Duraisamy G. Review of high efficiency and clean reactivity controlled compression ignition (RCCI) combustion in internal combustion engines. Prog Energy Combust Sci 2015;46:12–71.
[4] Verhelst S, Wallner T. Hydrogen-fueled internal combustion engines. Prog Energy Combust Sci 2009;35:490–527.
[5] Akansu SO, Dulger Z, Kahraman N, Veziroğlu TN. Internal combustion engines fueled by natural gas–hydrogen mixtures. Int J Hydrogen Energy 2004;29:1527–39.
[6] Ma F, Wang Y, Liu H, Li Y, Wang J, Ding S. Effects of hydrogen addition on cycle-by-cycle variations in a lean burn natural gas spark-ignition engine. Int J Hydrogen Energy 2008;33:823–31.
[7] Ma F, Wang Y, Liu H, Li Y, Wang J, Zhao S. Experimental study on thermal efficiency and emission characteristics of a lean burn hydrogen enriched natural gas engine. Int J Hydrogen Energy 2007;32:5067–75.
[8] Dai P, Chen Z, Chen S. Ignition of methane with hydrogen and dimethyl ether addition. Fuel 2014;118:1–8.
[9] Zhang Y, Huang Z, Wei L, Zhang J, Law CK. Experimental and modeling study on ignition delays of lean mixtures of methane, hydrogen, oxygen, and argon at elevated pressures. Combust Flame 2012;159:918–31.
[10] Yu G, Law CK, Wu CK. Laminar flame speeds of hydrocarbon + air mixtures with hydrogen addition. Combust Flame 1986;63:339–47.
[11] Halter F, Chauveau C, Djebaïli-Chaumeix N, Gökalp I. Characterization of the effects of pressure and hydrogen concentration on laminar burning velocities of methane–hydrogen–air mixtures. Proc Combust Inst 2005;30:201–8.
[12] Chen Z. Effects of hydrogen addition on the propagation of spherical methane/air flames: A computational study. Int J Hydrogen Energy 2009;34:6558–67.
[13] Hu E, Huang Z, He J, Zheng J, Miao H. Measurements of laminar burning velocities and onset of cellular instabilities of methane–hydrogen–air flames at elevated pressures and temperatures. Int J Hydrogen Energy 2009;34:5574–84.
[14] Vu TM, Park J, Kim JS, Kwon OB, Yun JH, Keel SI. Experimental study on cellular instabilities in hydrocarbon/hydrogen/carbon monoxide–air premixed flames. Int J Hydrogen Energy 2011;36:6914–24.
[15] Soo Kim J, Park J, Boong Kwon O, Ju Lee E, Han Yun J, In Keel S. Preferential diffusion effects in opposed-flow diffusion flame with blended fuels of CH4 and H2. Int J Hydrogen Energy 2008;33:842–50.
[16] Ying Y, Liu D. Detailed influences of chemical effects of hydrogen as fuel additive on methane flame. Int J Hydrogen Energy 2015.
[17] Ji C, Wang S. Effect of hydrogen addition on combustion and emissions performance of a spark ignition gasoline engine at lean conditions. Int J Hydrogen Energy 2009;34:7823–34.
[18] Ji C, Wang S. Combustion and emissions performance of a hybrid hydrogen–gasoline engine at idle and lean conditions. Int J Hydrogen Energy 2010;35:346–55.
[19] Ji C, Wang S. Experimental study on combustion and emissions performance of a hybrid hydrogen–gasoline engine at lean burn limits. Int J Hydrogen Energy 2010;35:1453–62.
[20] Tahtouh T, Halter F, Mounaïm-Rousselle C. Laminar premixed flame characteristics of hydrogen blended iso-octane–air–nitrogen mixtures. Int J Hydrogen Energy 2011;36:985–91.
[21] Bouvet N, Halter F, Chauveau C, Yoon Y. On the effective Lewis number formulations for lean hydrogen/hydrocarbon/air mixtures. Int J Hydrogen Energy 2013;38:5949–60.
[22] Mandilas C, Ormsby MP, Sheppard CGW, Woolley R. Effects of hydrogen addition on laminar and turbulent premixed methane and iso-octane–air flames. Proc Combust Inst 2007;31:1443–50.
[23] Jain S, Li D, Aggarwal SK. Effect of hydrogen and syngas addition on the ignition of iso-octane/air mixtures. Int J Hydrogen Energy 2013;38:4163–76.
[24] Bradley D, Cresswell TM, Puttock JS. Flame acceleration due to flame-induced instabilities in large-scale explosions. Combust Flame 2001;124:551–9.
[25] Bradley D, Hicks RA, Lawes M, Sheppard CGW, Woolley R. The measurement of laminar burning velocities and Markstein numbers for iso-octane–air and iso-octane–n-Heptane–air mixtures at elevated temperatures and pressures in an explosion bomb. Combust Flame 1998;115:126–44.
[26] Bradley D, Sheppart CGW, Woolley R, Greenhalgh DA, Lockett RD. The development and structure of flame instabilities and cellularity at low Markstein numbers in explosions. Combust Flame 2000;122:195–209.
[27] Law CK, Jomaas G, Bechtold JK. Cellular instabilities of expanding hydrogen/propane spherical flames at elevated pressures: theory and experiment. Proc Combust Inst 2005;30:159–67.
[28] Peters N. Turbulent combustion. Cambridge: Cambridge University Press; 2004.
[29] Chen Z. On the extraction of laminar flame speed and Markstein length from outwardly propagating spherical flames. Combust Flame 2011;158:291–300.
[30] Kee RJ, Grcar JF, Smooke MD, Miller JA. PREMIX: a program for modeling steady, laminar, one-dimensional, premixed flames. Sandia National Laboratory; 2000.
[31] Chen Z, Burke MP, Ju Y. Effects of Lewis number and ignition energy on the determination of laminar flame speed using propagating spherical flames. Proc Combust Inst 2009;32:1253–60.
[32] Chen Z. Effects of radiation and compression on propagating spherical flames of methane/air mixtures near the lean flammability limit. Combust Flame 2010;157:2267–76.
[33] Dai P, Chen Z, Chen S, Ju Y. Numerical experiments on reaction front propagation in n-heptane/air mixture with temperature gradient. Proc Combust Inst 2015;35:3045–52.
[34] Kee RJ, Lewis GD, Warnatz J, Coltrin ME, Miller JA. A Fortran computer code package for evaluation of gas-phase, multicomponent transport properties. Sandia National Laboratory; 1986.
[35] Kee RJ, Rupley FM, Meeks E, Miller JA. CHEMKIN-II: a Fortran chemical kinetics package for the analysis of gas-phase chemical and plasma kinetics. Sandia National Laboratory; 1996.
[36] Chen Z, Burke MP, Ju Y. On the critical flame radius and minimum ignition energy for spherical flame initiation. Proc Combust Inst 2011;33:1219–26.
[37] Yu H, Han W, Santner J, Gou X, Sohn CH, Ju Y, et al. Radiation-induced uncertainty in laminar flame speed measured from propagating spherical flames. Combust Flame 2014;161:2815–24.
[38] Zhang W, Chen Z, Kong W. Effects of diluents on the ignition of premixed H2/air mixtures. Combust Flame 2012;159:151–60.

[39] Chen Z, Burke MP, Ju Y. Effects of compression and stretch on the determination of laminar flame speeds using propagating spherical flames. Combust Theor Model 2009;13:343–64.
[40] Clavin P. Dynamic behavior of premixed flame fronts in laminar and turbulent flows. Prog Energy Combust Sci 1985;11:1–59.
[41] Chaos M, Kazakov A, Zhao Z, Dryer FL. A high-temperature chemical kinetic model for primary reference fuels. Int J Chem Kinet 2007;39:399–414.
[42] Curran HJ, Gaffuri P, Pitz WJ, Westbrook CK. A comprehensive modeling study of iso-octane oxidation. Combust Flame 2002;129:253–80.
[43] Li J, Zhao Z, Kazanov A, Dryer FL. An updated comprehensive kinetic model of hydrogen combustion. Int J Chem Kinet 2004;36:566–75.
[44] Chen Z, Dai P, Chen S. A model for the laminar flame speed of binary fuel blends and its application to methane/hydrogen mixtures. Int J Hydrogen Energy 2012;37:10390–6.
[45] Yamamoto K, Ozeki M, Hayashi N, Yamashita H. Burning velocity and OH concentration in premixed combustion. Proc Combust Inst 2009;32:1227–35.
[46] Cheng Y, Tang C, Huang Z. Kinetic analysis of H2 addition effect on the laminar flame parameters of the C1–C4 n-alkane–air mixtures: from one step overall assumption to detailed reaction mechanism. Int J Hydrogen Energy 2015;40:703–18.
[47] Tang CL, Huang ZH, Law CK. Determination, correlation, and mechanistic interpretation of effects of hydrogen addition on laminar flame speeds of hydrocarbon–air mixtures. Proc Combust Inst 2011;33:921–8.
[48] Wang H, Hahn TO, Sung CJ, Law CK. Detailed oxidation kinetics and flame inhibition effects of chloromethane. Combust Flame 1996;105:291–307.
[49] Sung CJ, Huang Y, Eng JA. Effects of reformer gas addition on the laminar flame speeds and flammability limits of n-butane and iso-butane flames. Combust Flame 2001;126:1699–713.
[50] Di Sarli V, Benedetto AD. Laminar burning velocity of hydrogen–methane/air premixed flames. Int J Hydrogen Energy 2007;32:637–46.
[51] Hirasawa T, Sung CJ, Joshi A, Yang Z, Wang H, Law CK. Determination of laminar flame speeds using digital particle image velocimetry: binary fuel blends of ethylene, n-butane, and toluene. Proc Combust Inst 2002;29:1427–34.
[52] Liu X, Ji C, Gao B, Wang S, Liang C, Yang J. A laminar flame speed correlation of hydrogen–methanol blends valid at engine-like conditions. Int J Hydrogen Energy 2013;38:15500–9.
[53] Fu J, Deng B, Wang Y, Yang J, Zhang D, Xu Z, et al. Numerical study and correlation development on laminar burning velocities of n-butanol, iso-octane and their blends: Focusing on diluent and blend ratio effects. Fuel 2014;124:102–12.
[54] Ji C, Liu X, Wang S, Gao B, Yang J. A laminar burning velocity correlation for combustion simulation of hydrogen-enriched ethanol engines. Fuel 2014;133:139–42.
[55] Sileghem L, Alekseev VA, Vancoillie J, Nilsson EJK, Verhelst S, Konnov AA. Laminar burning velocities of primary reference fuels and simple alcohols. Fuel 2014;115:32–40.
[56] Zhang Y, Yang Y, Miao Z, Zhang H, Wu Y, Liu Q. A mixing model for laminar flame speed calculation of lean H2/CO/air mixtures based on asymptotic analyses. Fuel 2014;134:400–5.
[57] Sankaran Ramanan, Im HG. Effects of hydrogen addition on the Markstein Length and flammability limit of stretched methane/air premixed flames. Combust Sci Technol 2006;178:1585–611.
[58] Kim HH, Won SH, Santner J, Chen Z, Ju Y. Measurements of the critical initiation radius and unsteady propagation of n-decane/air premixed flames. Proc Combust Inst 2013;34:929–36.
[59] Zhang H, Chen Z. Spherical flame initiation and propagation with thermally sensitive intermediate kinetics. Combust Flame 2011;158:1520–31.
[60] Chen Z. On the accuracy of laminar flame speeds measured from outwardly propagating spherical flames: methane/air at normal temperature and pressure. Combust Flame 2015;162:2242–53.